11th CIRP Conference on Photonic Technologies [LANE 2020] on September 7-10, 2020

Influence of the surface roughness and pulse energy in the production of dimple features on Cr₂O₃ surfaces

Juan Ignacio Ahuir-Torres[a],*, Martin Sharp[a] and Mehdi Seddighi[b]

[a]General Engineering Research Institute, Faculty Engineeringadn Technology, Liverpool John Moores University, GERI Building, 3 Byrom Street, Liverpool and L3 3AF, United Kingdom
[b]Maritime and Mechanical Engineering, Faculty of Engineering and Technology, Liverpool John Moores University, James Parsons Building, 3 Byrom Street, Liverpool and L3 3AF, United Kingdom

* Corresponding author. Tel.: +44-151-231-2031. *E-mail address:* j.i.ahuirtorres@ljmu.ac.uk

Abstract

Laser dimple generation can functionalise ceramic surfaces. Dimple characteristics determine the functionalised surface properties, which has numerous applications. Laser parameters and material properties are key factors in the design of the dimple features. Pulse energy, E_p, and average surface roughness, Ra, are important parameters in the dimple production. Thus, the influence of the E_p of InfraRed (IR) nanosecond pulsed laser on the dimple characteristics generated on two Cr₂O₃ surfaces (as-received and polished) are studied in this work. The increase of the E_p increased the dimples features (Diameter, D, and depth, L). Polished surfaces gave dimples with increased depth while dimples produced on as-received samples were shallow. The energy fluence ablation threshold, φ_{th}, is higher for as-received surface than for polished Cr₂O₃.

Keywords: Surface roughness; pulse energy; laser texturing; Cr₂O₃; nanosecond pulsed laser

1. Introduction

The production of dimples on material surfaces via laser processing is a good tool to improve the surface properties of ceramic materials. The characteristics of the dimples (type, shape, depth, diameter and width) determine the textured surfaces properties, leading to a number of potential industrial applications. The laser parameters and the physicochemical properties of the materials are key factors in the design of the dimple features [1].

Pulse energy, E_p, and roughness, Ra, are essential parameters in the production of the dimples on ceramic materials. The increase of E_p commonly enlarges the size of the dimple characteristics (diameter, D, and depth, L,) [2,3]. Certain high E_p can nevertheless create narrower and shallower dimples than the dimples produced at low or moderate E_p. This is due to the plasma shielding effect that

absorbs and/or reflects part of the laser radiation [4]. On the other hand, the increasing of Ra usually enhances the absorption of the laser energy by the material [5]. However, an excessive Ra can diminish the laser energy density absorbed by the surface [2]. Furthermore, laser processing can modify the chemical composition of the ceramic materials at certain conditions [6,7]. This can degrade the physicochemical properties of the material functionalised with dimples.

In respect of the type of lasers employed, nanosecond pulsed lasers are widely utilised in the production of surface textures, e.g. grooves or dimples, because they deliver beneficial properties, such as reduced heat affected zone, HAZ, and recast layer thickness [8].

In the literature [7,8], the production of dimpled surfaces on ceramic coatings using pulsed lasers has been extensively studied. Nonetheless, the studies about the influence of these

parameters for nanosecond pulsed lasers on dimples characteristics on Cr_2O_3 are rare.

For these reasons, the present work studies the influence of E_p and R_a on the characteristics of the dimples on Cr_2O_3 coatings. The Cr_2O_3 coatings were produced using atmospheric plasma spray, APS. The dimples were produced on Cr_2O_3 coatings with two distinct surface conditions, as-received and subsequently polished, via single shots generated with an IR (1064nm) nanosecond (200ns) pulsed fibre laser operating at various E_p (80µJ-800µJ). The surface morphology of the samples were evaluated through scanning electron microscopy, SEM. The influence of the E_p and Ra on D and L was featured via characterisation of the shape and the topography of the samples with an optical profilometer. The chemical composition of the samples were analysed via energy dispersive spectroscopy, EDS.

Nomenclature

IR   Infrared
E_p Pulse Energy
HAZ   Heat Affected Zone
SEM   Scanning Electron Microscopy
SE   Secondary Electrons
EDS   Energy Dispersive Spectroscopy
d_o Experimental focused beam size
E_{th} Energy ablation threshold
φ_{th} Energy fluence ablation threshold
APS   Atmospheric Plasma Spray
Ra   Average roughness of surface
Cr_2O_3 Dichromium trioxide
D   Diameter of the dimple
L   Depth of the dimple
$d_{o(Theo)}$ Theoretical focused beam size
l   Energy depth of penetration

2. Experimental Setup

The laser was an IR fibre laser (*redENERGY, model SP-20P-0202-001, Serial Number 324466*) that was supplied by *SPI Laser UK Limited*. The laser beam was expanded to 5.73mm diameter by beam-expander *2-8X, 1064nm, serial number 4401-256-00-20*, supplied by *Linos*. The laser beam was manipulated by a scanning galvanometric mirror, *Nutfield Technology, Inc*. model *3XB*. The scanning galvanometer mirror was controlled via *SAMLight 3.05* software. The laser beam was focused using a f-Theta lens of 100mm focal length, *F-Theta-Ronar, f=100mm, 1064nm, serial number 4401-302-000-20/21*, supplied by *Linos (Qioptiq)*. The samples were placed on the four axis automatic table, *PRO115-05MM-100-TTM-9DU-NC BMS-BRK-3-C025-NO PLOTS, serial number 148797-B-1-1* supplied by *Aerotech*. This automatic table was controlled by mean of *NView (v2.22)* from *Aerotech*. The dimples were created on the Cr_2O_3 coatings through single shots using the laser parameters that are detailed in Table 1.

Table 1. Details of the selected laser parameters to produce the dimples on the Cr_2O_3 surfaces.

Parameter	Value
Wavelength(nm)	1064
Pulse length (ns)	200
TEM	00
Focal length (mm)	100.00
Raw beam size (mm)	5.73
Quality of beam (M^2)	2.14
Pulse frequency (kHz)	25
Atmosphere	Air
$d_{o(Theo)}$ (µm)	50.88
Number of pulses per dimple	1
E_p (µJ)	40, 80, 160, 240, 320, 400, 480, 560, 640, 720 and 800

The surfaces of the Cr_2O_3 coatings before laser processing were as-received (without previous surface treatment) and polished (mirror-to-polishing). The details of the coatings are summarized in Table 2.

Table 2. Details of the Cr_2O_3 coating fabrication and Ra of the as-received and polished surfaces.

Parameter	Detail	
Fabrication technique	Atmospheric Plasma Spray (APS)	
Powder Size (µm)	25±10	
Current (A)	480	
Ar Flow (l/min)	62	
H_2 Flow (l/min)	5	
Thickness (µm)	300	
Substrate	Mild steel (AISI 1040 Steel)	
Ra (µm)	As-received	4.400±0.500
	Polished	0.160±0.010

The geometry, morphology and chemical composition of the samples were evaluated via surface analysis techniques; SEM, optical profilometry and EDS. The SEM analyses of the samples were using a Schottky field emission electron microscope supplied by *Thermo Fisher Scientific* model *Quant 200 ESEM*. The electron microscope was controlled through *Inca* software. The SEM pictures were conducted at 1000X magnification, 45pA of tension current, 15-20KV of potential acceleration, $1.92*10^{-4}$ bar of pressure and with SE. The optical profiler was *ContourGT, model 1009049,* supplied by *Bruker*. Bruker *Vision64* software was used to control the instrument. The optical profiling was carried out with green light at 10X magnifications and 1Pixel/µm. The electron microscope was also utilised to conduct the EDS analyses on the samples and its working conditions were the same as for the SEM analyses. The spectrums of EDS were evaluated via *Inca* software.

3. Results and discussion

The SEM pictures with SE of the samples can be seen in Fig. 1. All samples had imperfections, as cracks and pores, but

their origins were dissimilar. The surface imperfections of the as-received (Fig.1.a.) and polished (Fig.1.c.) samples exist before laser processing (surfaces before laser dimpling) being generated during the creation of the coating. The defects of the dimples produced on as-received (Fig.1.b.) and polished surfaces (Fig.1.d.) are produced during laser processing. The dimple cracks are created by thermal stresses that are caused by fast solidification of the melted material generated by laser processing [6,8]. Pores are produced through air trapped by the melted material [9].

The morphology of the dimples depends on the surface status of the coatings before laser processing. The surface within the dimples on the as-received surface are smoother (Fig.1.b.) than the non-processed areas of the as-received samples (Fig.1.a.). This indicates that single shots principally melted the as-received surfaces [6]. In addition, the ablation for these coatings is the normal boiling mechanism because melting is the main thermal process [3]. In regard of polished surfaces, ejected melted material is observed outside of the dimples (Fig.1.d.). This showed the ablation mechanism is phase explosion [4]. The nucleation, growth and subsequent explosion of the liquid-gas bubble characterise the phase explosion. Molten material is ejected by the explosion of this bubble and is deposited nearby [4].
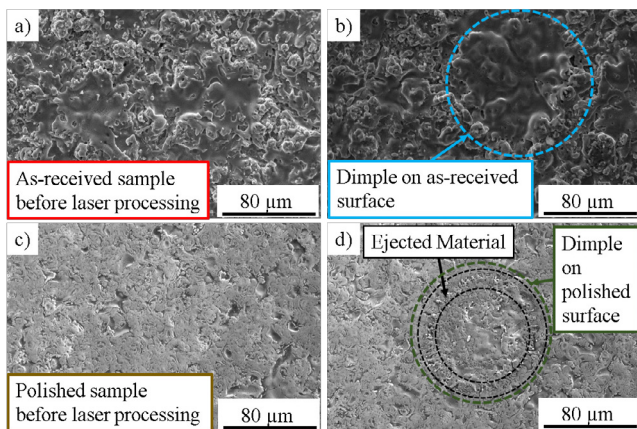

Fig. 1. SEM pictures with SE at 1000X magnifications of the as-received surface a), and polished surface c) and, the dimples produced at 800µJ with 200ns single shot on the b) as-received and d) polished surfaces.

The influence of E_p and of Ra on dimple diameter, D, can be viewed in Fig. 2. The increase of E_p increased D for both surfaces (Fig.2.a.). This is due to energy spatial distribution of the laser beam being Gaussian [3]. The dimples at same E_p on both coatings had similar D. The single shots at ≥400µJ produced dimples on as-received surfaces (Ra=4.400±0.500µm) whilst the single shots at ≥240µJ created the dimples on polished surfaces (Ra=0.160±0.010µm). This can indicate that φ_{th} for polished surfaces is lower than for as-received surfaces. This can be due to the reduction of the laser energy density on surfaces because the topographic characteristics of the as-received surfaces [5]. This is discussed later.

Experimental focused spot diameter, d_o, and energy ablation threshold, E_{th}, were estimated via the combination of Fig. 2.b. with equation 1 [2,3].

$$D^2 = d_o^2 * ln(E_p) - d_o^2 * ln(E_{th}) \tag{1}$$

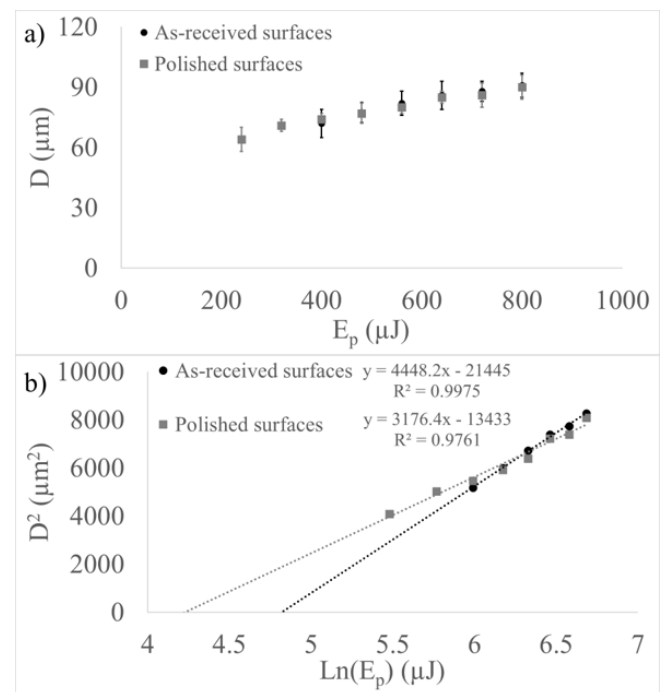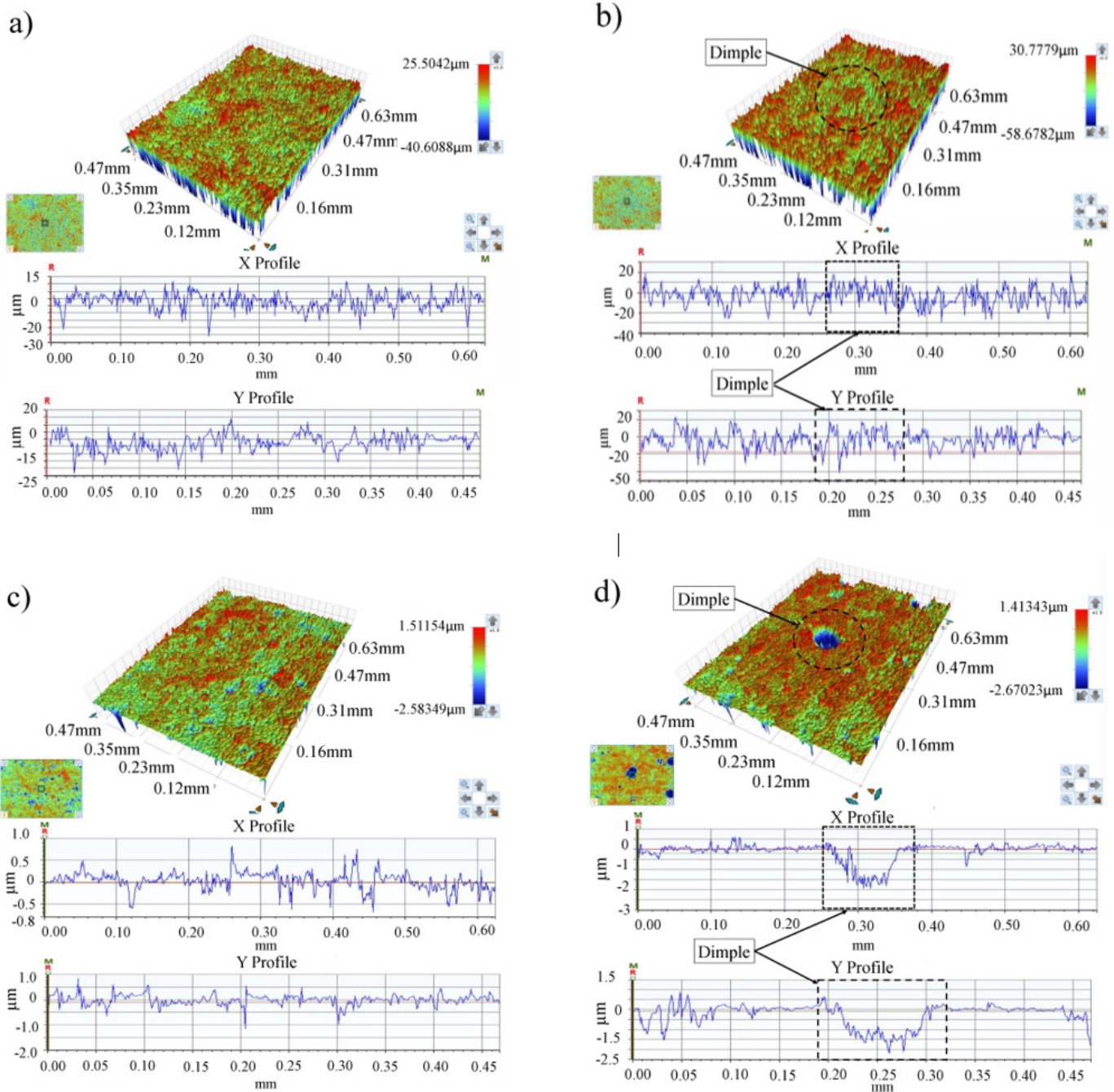Fig. 2. Graph of a) D vs E_p and b) D^2 vs $Ln(E_p)$

Fig. 3. 3D pictures and profiles obtained with optical profiler at 10X magnification and with green light of the as-received surface a) and polished surface c) before laser processing and, the dimples created at 800μJ with 200ns single shot on the as-received surface b) and polished surfaces d)

The d_o of the polished coating (56.36μm) was similar to $d_{o(Theo)}$ (50.88μm). However, d_o of the dimples on as-received surfaces (65.75μm) was larger than $d_{o(Theo)}$. This is due to relief of the as-received surfaces scattering the laser radiation out of the laser beam. This increases the effective surface area of the laser radiation on sample [2]. E_{th} of the as-received coating (119.83μJ) was higher than for polished surfaces (68.65μJ). Greater effective surface area requires a higher E_p to begin ablation because the effective spot size is larger [2]. φ_{th} were determined through the combination of E_{th} with the equation 2.

$$\varphi_{th} = \frac{4 * E_{th}}{\pi * d_o^2} \qquad (2)$$

φ_{th} was higher for cases of the production of dimples on as-received surfaces (3.53J/cm^2) than for the dimples on polished surfaces (2.75J/cm^2). This is logical by the wider effective surfaces area of the as-received surfaces [2].

Topography and profiles of the samples can be observed in Fig. 3. The dimple topography on the as-received surface (Fig.3.b.) is similar to the topography of the as-received surfaces (Fig.3.a.) that were characterised by a coarse relief. This indicates that the depth of removed material of the dimples was minimum for as-received surfaces. This suggests the ablation mechanism of normal boiling features, as it has a lower ablation rate in depth than other ablation mechanisms (e.g. phase explosion) [3]. Thus, shallow dimples are produced on the as-received surfaces via the normal boiling mechanism.

The dimples on polished surfaces (Fig.3.d) were surrounded by a crest and had a basin in the centre. The crests were formed by the fast re-solidification of the recast material that is accumulated on the dimple rims by the evaporated material pressure on the molten material [10]. The valley is generated by explosion of the bubble in the phase explosion [4]. The dimple shapes were of a spherical cap that is identified as U-type [11].

The dissimilar ablation mechanisms according to surface status is due to different amount of energy density absorbed by the coatings according to surface status. The phase explosion requires more energy density than the normal boiling [4, 12]. The as-received surfaces absorb less energy density than the polished surfaces because its effective surface area is larger. High Ra produces a greater effective area [2]. Thus, at the same E_p, the low energy density ablation mechanism, normal boiling, occurs on the as-received surfaces. The ablation mechanism of high energy density, phase explosion, is produced on polished surfaces.

The diameter, D, and depth, L, of the dimple features produced on the polished surfaces with varying pulse energies, E_p, is shown in Fig. 4. The values of D and L increase with increasing E_p (Fig.4.a). This is expected as these characteristics are proportional to E_p, according to the equations 1 (D) and 3 (L) [3]:

$$L = l * ln(E_p) - l * ln(E_{th}) \qquad (3)$$

d_o, E_{th} and l were calculated using the line fits of Fig. 4.b with the equations 1 and 3. Experimental beam diameter, d_o, was calculated as 60.12μm and is similar to the previously calculated d_o (56.36μm) and the theoretically calculated focussed beam diameter, $d_{o(Thoe)}$ (50.88μm). Threshold pulse energy, E_{th}, is calculated as 136.33μJ and is higher than the previously estimated E_{th} (68.65μJ). This E_{th} is calculated corresponding to the evaporation process, while the previously calculated value is for the melting regime. The evaporation process requires more energy to occur than the melting process. The energy depth of penetration, l, was calculated as 1.183μm.

The Ra of the dimples were higher than that of the surfaces before laser dimpling, for example, in the polished samples (Fig.4.c.), which indicates that the generation of the dimples has a roughness effect on Cr_2O_3 coatings. Ra nevertheless had unclear pattern with E_p.

The chemical composition of the sample was analysed using EDS. The polished sample results are shown in Fig. 5. The concentrations of the chromium and oxygen within the dimples were found to be similar to the surfaces before laser dimpling, for both samples (as-received and polished). This indicates that the single shots do not modify the chemical composition of the original coatings.

4. Conclusions

This paper presented a study about the influence of E_p and Ra on dimple features produced on Cr_2O_3 coatings. This was achieved via the analyses of the dimples produced with 200ns IR laser single shots at various E_p (0.080-0.800J) on as-

received (high Ra) and polished (low Ra) surfaces. The knowledge obtained in this study allows the design of the dimples on two surfaces with dissimilar features.
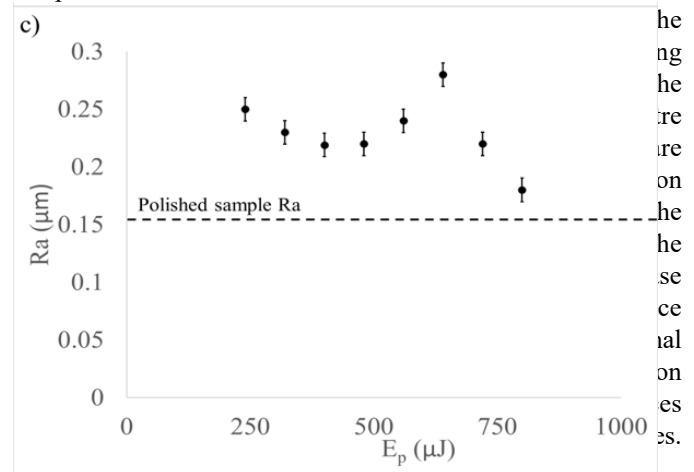

Fig. 4. Graphs of the dimple characteristics produced on the polished surfaces as functions of E_p. a) D and L vs E_p, b) D^2 and L vs $Ln(E_p)$ and, c) Ra of the samples depending on E_p .
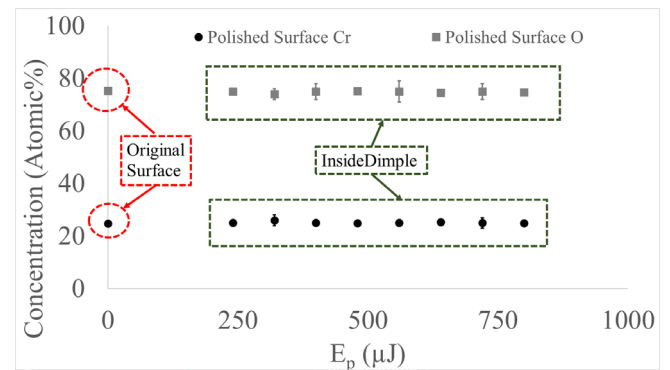

Fig. 5. Graph of chemical composition (atomic %) as function E_p of the polished surfaces.

Different ablation mechanisms arise as the energy density absorbed by coating is different depending on the surface roughness, Ra. As-received surfaces have lower energy density than polished surfaces because the focused laser spot is absorbed over a larger effective area. In addition, the energy density is inversely proportional to laser effective area. On the other hand, phase explosive needs more energy density than normal boiling. Phase explosion therefore occurs on polished surfaces while normal boiling occurs on the as-received surfaces. Besides, this indicates that laser processing is more efficient on the polished surface than the as-received surface because its energy density is, in effect, higher.

The diameter, D, and depth, L, of the dimples can be determined through the selection of the pulse energy, E_p. The increasing of E_p widens and deepens the dimple for polished surfaces. In the case of D, this is due to the Gaussian spatial distribution of the energy in laser beam. In respect of L, this is because the ablation rate usually is proportional to E_p. In addition, the influence of E_p on the dimple features for each coating has been quantified with the threshold fluence, φ_{th}, and energy depth of penetration, l, This allows the design of

textures with dissimilar feature dimensions to the dimples presented here through the use of equations 1 and 3.

The chemical composition within the dimples are similar to the original coating chemical composition. So the production of a dimpled surface on this coating should maintain the high chemical inertness of Cr_2O_3, this is one of the main advantage of this material.

Hence, the manufacture of dimpled surfaces, of this scale, with specified diameter and depth, can be created via single shots of the 200ns IR fibre laser on Cr_2O_3 coatings, without chemical modifications, using a suitable combination of the pulse energy, E_p, with surface roughness, Ra.

Acknowledgements

Uncategorized References

[1] Wahab J, Ghazali MJ, Yusoff WMW, Sajuri Z. Enhancing material performance through laser surface texturing: A review. Trans. IMF. 2016;94:193-8.
[2] Mustafa H, Mezera M, Matthews DTA, Römer G. Effect of surface roughness on the ultrashort pulsed laser ablation fluence threshold of zinc and steel. Appli. Surf. Sci. 2019;488:10-21.
[3] Mannion P, Magee J, Coyne E, O'connor G, Glynn T. The effect of damage accumulation behaviour on ablation thresholds and damage morphology in ultrafast laser micro-machining of common metals in air. Appl. Surf. Sci. 2004;233:275-87.
[4] Jafarabadi MA, Mahdieh MH. Investigation of phase explosion in aluminum induced by nanosecond double pulse technique. Appl. Surf. Sci. 2015;346:263-9.
[5] Fu Y, Li J, Liu Y, Liu L, Zhao H, Pan Y. Influence of surface roughness on laser-induced damage of Nd: YAG transparent ceramics. Ceram. Int. 2015;41:12535-42.
[6] Shankar AR, Babu BJ, Sole R, Mudali UK, Khatak H. Laser remelting of plasma sprayed zirconia based ceramic coating for pyrochemical reprocessing applications. Surface engineering. 2007;23:147-54.
[7] Lahoz R, de la Fuente GF, Pedra JM, Carda JB. Laser engraving of ceramic tiles. Int. J. of Appl. Ceram. Technol. 2011;8:1208-17.
[8] Rihakova L, Chmelickova H. Laser micromachining of glass, silicon, and ceramics. Adv. in Mater. Sci. and Eng. 2015;2015.
[9] Sola D, Conde A, García I, Gracia-Escosa E, De Damborenea JJ, Peña JI. Microstructural and wear behavior characterization of porous layers produced by pulsed laser irradiation in glass-ceramics substrates. Materials. 2013;6:3963-77.
[10] Xing Y, Deng J, Feng X, Yu S. Effect of laser surface texturing on Si3N4/TiC ceramic sliding against steel under dry friction. Mater. Des. (1980-2015). 2013;52:234-45.
[11] Nanbu T, Ren N, Yasuda Y, Zhu D, Wang QJ. Micro-textures in concentrated conformal-contact lubrication: effects of texture bottom shape and surface relative motion. Tribol. Lett. 2008;29:241-52.
[12] Sinha S. Thermal model for nanosecond laser ablation of alumina. Ceram. Int. 2015;41:6596-603.